

# ACTIVE MICRO-MIXING BY REGENERATION OF ARTIFICIAL TURBULENT STRUCTURES

Sedat Tardu and Rabie Nacereddine

Laboratoire des Ecoulements Géophysiques et Industriels (LEGI)

B.P. 53 X 38041 Grenoble, Cédex, France

Sedat.Tardu@hmg.inpg.fr

## ABSTRACT

An active micro-mixing strategy through forcing the flow by synthetic wall jets is proposed. It is based on the interaction of induced streamwise vortices in a specific way. There is a spanwise shift between two quasi-streamwise vortices in such a way that one of them compresses the wall normal vorticity layer created by the other, leading to the generation of new wall normal vortical structures. The latter are subsequently tilted by the shear to give birth to new small-scale longitudinal active structures that are efficient in mixing. The feasibility of this strategy is shown through direct numerical simulations of high spatial and temporal resolution.

## INTRODUCTION

The importance of developing efficient mixing strategies in microsystems is obvious. The success of the commercial micro devices depend most of the time on their capability of mixing. The existing passive and active micro-mixers are often confronted to the tradeoff between transport and mixing, excellent mixing leading sometimes to a poor transport (Tian et al., 2005; for a review of micromixers see Hessel et al., 2005). The mixing in micro-channel flows purely depends on the diffusion process, which is slow. Existing micro-mixers involve phenomena related to lamination, external stirring, chaotic advection using for example microchannels with patterned grooves. The micro-mixers can also be classified as active or passive.

Most of the strategies used in micro-mixing deal with mixing in a large spatial extend. Most of the time, mixing in a very localized part of the flow is required. Best mixing in this sense is of course induced by local turbulence that cannot be (unfortunately) achieved in typical micro-flows. The aim here therefore is to find a way to mimic wall turbulence "synthetically" at very low Reynolds numbers of the order of one. Structures responsible for the wall turbulence are the quasi-streamwise vortical (QSS) structures. The generation of these structures is still not well understood. In a recent paper we proposed a new mechanism based on the interactions and self-reproduction of these structures (Tardu and Nacereddine, 2006). This mechanism will be shortly discussed first in the next session. The efficiency of the mixing achieved by imposing a spanwise asymmetry between two vortical structures will then be shown first for a high laminar Reynolds number flow, through well-resolved direct numerical simulations. The method will subsequently be applied to a microchannel flow with significantly small Reynolds number, wherein

two spanwise asymmetric perturbations whose intensities vary periodically in time are superimposed to the flow. We will discuss the technical feasibility of this mixing strategy in the last session.

## BY-PASS TRANSITION THROUGH INTERACTION OF LOCALIZED PERTURBATIONS

One of the main characteristics of by-pass transition is the generation of quasi-streamwise vortical structures (QSS) near the wall at the late spatial and temporal development stages of a localized perturbation (Henningson et al., 1993). The main generation term in the streamwise vorticity  $\omega_x$  generation equation is the production term resulting from the tilting of wall normal vorticity by the shear that reduces to  $-\frac{\partial w}{\partial x} \frac{\partial \bar{u}}{\partial y}$  where  $\frac{\partial w}{\partial x}$  is the streamwise gradient of the spanwise velocity and  $\frac{\partial \bar{u}}{\partial y}$  is the mean shear. Here  $x, y, z$

are respectively the streamwise wall normal and spanwise coordinates with the corresponding velocity components  $u, v, w$ . The base flow is a Poiseuille flow with the streamwise velocity distribution  $\bar{u}(y)$ . The set-up of the  $x$  dependence is problematic. A streamwise dependence is hardly conceivable in the immediate vicinity of the quite elongated quasi-streamwise vortices. Tardu (1995) proposed a mechanism that may lead to the QSS generation through interactions of existing structures with the wall normal vorticity layers generated by the QSS themselves (Jiménez, 1994). Consider the conceptual model given in Fig.1 that shows two pairs of counter rotating vortices labeled respectively by  $A$  and  $B$ . Walls of normal vorticity layers  $\omega_y$  are generated behind the vortices resulting from the kinematics induced by the near wall velocity distribution (Jiménez, 1994). One may rigorously show by making use of the Biot-Savart law that the streamwise variations of the spanwise velocity component are related to

$$\frac{\partial w}{\partial x} \propto \frac{1}{4\pi} \int_{-\infty}^0 dz' \int_{-\infty}^{+\infty} \Delta(x', z', t) \log \left[ (x-x')^2 + (z-z')^2 \right] dx' \quad (1)$$

where

$$\Delta(x', z', t) = \frac{\partial^2 \omega_y^+}{\partial x'^2} - \left| \frac{\partial^2 \omega_y^-}{\partial x'^2} \right| \quad (2)$$

represents the dissymmetry between the streamwise variations of the positive and negative wall normal vorticity layers shown in Fig. 1. The details are omitted here and can be found in Tardu and Nacereddine (2007) and Tardu et al. (2007), but it is clear that a dissymmetry  $\Delta(x', z', t)$  is obviously necessary to regenerate  $\frac{\partial w}{\partial x}$  which in return may lead to new quasi-streamwise structures. The compression of one of the vorticity layers  $\omega_{y \pm A}$  by the large positive straining induced by the left counterrotating vortex  $B$  in Fig. 1 may break up the symmetry and enhance the by-pass transition. It can be shown that for sufficiently large times the local dimensionless vorticity disappears exponentially in time according to  $\omega_{y+A}^* \propto \exp(-\gamma^* t^*)$  under the stagnation flow with parameter  $\gamma^*$  induced by the sweep motion. The negative  $\omega_{y-A}^*$  sidewall in return, is located far away from the stagnation flow. It is primarily under the effect of viscosity. The maximum vorticity in this layer decreases therefore as  $\omega_{y-A}^* \propto \frac{1}{\sqrt{t^*}}$ . For typically  $t^* \gg \frac{2}{\gamma^*}$  the positive vorticity disappears almost instantaneously giving rise to a large  $\frac{\partial w}{\partial x} > 0$  wall layer that can subsequently be tilted by the shear and roll up to a new streamwise structure. The mechanism is detailed in Tardu, Nacereddine (2007) and Tardu et al. (2007). The aim of the present study is to investigate the impact of this regeneration concept on the mixing in micro-channel flows at significantly low Reynolds numbers.

## DIRECT NUMERICAL SIMULATIONS AND INITIAL CONDITIONS

The channel DNS code of Orlandi (2001) has been adapted for the present purpose. The number of computational modes is  $256 \times 128 \times 128$  in respectively streamwise, wall normal and spanwise directions. The sizes of the computational domain extend from  $16\pi a$  in  $x$ ,  $2a$  in  $y$  and to  $8\pi a$  in  $z$  where  $a$  stands for the half height of the channel. Stretched coordinates are used in the wall normal direction. Hereafter the quantities are normalized with respect to  $a$  and the centerline velocity of the Poiseuille base flow.

Two pairs of counter rotating vortices have been injected in the channel flow with streamfunctions of the form:

$$\psi = \varepsilon f(y) \left( \frac{x'}{l_x} \right) z' \exp \left[ - \left( \frac{x'}{l_x} \right)^2 - \left( \frac{z'}{l_z} \right)^2 \right] \quad (3)$$

where  $x' = x \cos \vartheta - z \sin \vartheta$ ,  $z' = x \sin \vartheta - z \cos \vartheta$  and  $\vartheta$  is the angle of the perturbation which has been set to  $\vartheta = 0$  here. The perturbation flow field is given by :

$$(u, v, w) = (-\psi_y \sin \vartheta, \psi_{z'}, -\psi_y \cos \vartheta) \quad (4)$$

and  $f(y) = (1+y)^p (1-y)^q$ . This is the same type of perturbation used by Henningson et al. (1993). The difference here, however is in the modeling of the configuration given in Fig. 1. We combined two different  $\psi$  respectively for the structures  $A$  and  $B$  and shifted  $B$  in the  $z$  plane. More clearly we have chosen  $p_A = q_A = 2$ ,

$\varepsilon_A = 0.1$ ,  $l_{xA} = l_{zA} = 4$  for the structure  $A$  which is consequently centered at the centerline of the channel. The streamfunction corresponding to the structure  $B$  is of the same form but shifted in the spanwise direction by  $\delta$  i.e.

$$\psi_B = \varepsilon_B f_B(y) \left( \frac{x'}{l_x} \right) (z' + \delta) \exp \left[ - \left( \frac{x'}{l_x} \right)^2 - \left( \frac{z' + \delta}{l_z} \right)^2 \right] \quad (5)$$

The perturbation parameter and  $p$  and  $q$  are chosen in such a way that  $B$  is closer to the wall and interacts sufficiently strongly with the wall vorticity layers generated by  $A$ . Thus,  $p_B = 1.5, q_B = 6$ ,  $\varepsilon_B = 0.02$  and  $l_{xB} = l_{zB} = 2$  and  $B$  is centered at  $y = -0.6$  ( $y = 0$  is the centerline, and  $y = -1$  is the upper wall). The imposed streamfunction is  $\psi_A + \psi_B$ . The perturbation parameters  $\varepsilon_A$  and  $\varepsilon_B$  are chosen in such a way that  $A$  and  $B$  cannot *individually* trigger the by-pass transition as it will be shown in the next session.

The simulation of passive scalar transport, is performed through the resolution of the equation:

$$\frac{\partial T}{\partial t} + \frac{\partial (u_j T)}{\partial x_j} = \frac{1}{RePr} \frac{\partial^2 T}{\partial x_j^2} \quad (6)$$

where  $Pr$  is the Prandtl number. The resolution of this equation requires the calculation of the velocity field at the same time. So, the Direct Numerical and Heat transfer simulations have to be performed simultaneously. The numerical complexity is quite similar to the DNS resolution and similar tools can be employed. A, Runge-Kutta (3<sup>rd</sup> order) scheme is applied for the time advancement while the diffusive term is resolved by a direct LU decomposition. The numerical cost of the heat transfer resolution is quite low and corresponds approximately to 1/5 of the DNS one.

## RESULTS

To give some insights into the interactive regeneration process, we will first briefly discuss some results emerging from a steady forcing with constant  $\varepsilon_A$  and  $\varepsilon_B$  and a high Reynolds number of  $Re = 2000$ . The evolution of the total energy  $E_{tot} = \iiint_V (u^2 + v^2 + w^2) dV$ , is shown in Fig.2 in

this case. It is computed over the computational volume  $V$  and divided by the initial energy  $E_{tot i}$ . It is seen in Fig. 2 that the energy increases continuously by a factor of 35 at  $t = 200$  when  $A$  is combined with  $B$  while the energy associated with  $A$  and  $B$  decreases to zero after the initial algebraic stage at  $t \geq 100$ .

The regeneration of the structures cannot be maintained at low Reynolds numbers when they result from initial perturbations. The Poiseuille flow is indeed absolutely stable for  $Re < 1000$ . Thus, the mixing at low Reynolds numbers can be guaranteed only if the flow is forced somehow. In the frame of the present philosophy, the regeneration of synthetic turbulent like structures can be maintained by generated by spanwise localized unsteady blowing/suction that are easy to realize by means of microsystems. The simulation of the oscillating synthetic wall jets can be achieved by time modulating the strength of

the perturbations  $\varepsilon_A$  and  $\varepsilon_B$  appearing in the equation (3). More specifically we took:

$$\begin{aligned}\varepsilon_A(t) &= a_A \sin\left(\frac{2\pi}{T_A}t + \varphi_A\right) \\ \varepsilon_B(t) &= a_B \sin\left(\frac{2\pi}{T_B}t + \varphi_B\right)\end{aligned}\quad (7)$$

The amplitudes are quite small in this case, with  $a_A = 10^{-3}$  and  $a_B = 2 \cdot 10^{-4}$ . Before presenting the results for particularly small Reynolds numbers, we will show first the feasibility of this process for a large Reynolds number of  $Re = 1500$ . The imposed period is  $T_A = T_B = 12$ . Fig. 3 shows the evolution of the energy associated with the wall normal velocity component  $v$  versus time for the interactive combination  $A+B$  and for  $A$  and  $B$  alone. It is clearly seen in this Fig. that the energy increases significantly for  $t \geq 60$  in case  $A+B$ . The triggering of the bypass transition mechanism takes place through the generation of new wall normal vorticity that lead to small-scale quasi-streamwise structures that are the best candidates for mixing. Fig. 4 shows the contours of  $\lambda_2$  events (Jeong and Hussein, 1995) representing stretched quasi-streamwise vortices at  $t = 100$ . Note the strong agglomeration of the structures in the interaction zone  $z < 0$  in the case  $A+B$  (Fig.4a), compared with only few and weak structures in the case  $A$  only (not shown) and  $B$  (Fig. 4b).

Having shortly shown the efficiency of the proposed mechanism we now go through the discussion of the results obtained at a significantly low Reynolds number  $Re = 10$  representing the mixing process in a mini-micro channel. Note that there is no apparent reason for some limitation in the Reynolds number and the choice  $Re = 10$  has been made only to limit the computational time cost. In order to resolve the characteristics of *precisely localized* transport of the scalar  $T$  we use as initial conditions a profile of the form:

$$\begin{aligned}T &= T_1 \exp(-r) & \text{for } r \leq 1 \\ T &= T_2 = T_1 \exp(-1) & \text{for } r \geq 1\end{aligned}$$

where  $r^2 = \left(\frac{x}{l_x}\right)^2 + \left(\frac{y}{l_y}\right)^2 + \left(\frac{z}{l_z}\right)^2$ . That typically

represents a concentrated bubble (Fig. 5, at the right top). The results have been obtained here with  $l_x = l_z = 30$  and  $l_y = 0.2$ . The imposed period is  $T_A = T_B = 15$ , while the amplitudes now are larger,  $a_A = a_B = 0.009$ . Fig. 5 shows snapshots of the scalar distribution at approximately half of the oscillation period for the configuration  $A+B$  and  $B$  alone. Immediately after the beginning of the imposed forcing (Fig.5a), the mixing becomes efficient in the zone  $-10 < z < 0$  wherein the interactions of  $A$  with  $B$  take place as early as  $t = 1$ . The mixing is practically achieved at downstream of the imposed perturbation at  $x \geq 0$  but also upstream at  $x \leq -2$  (Fig.5a). The structure  $A$  alone hardly intervenes in the mixing process, and the effect of  $B$  alone is shown in Fig. 5b to be compared with 5a to better appreciate the efficiency of the mechanism suggested here. At  $x = 1$  for instance the mixing is only poor under the single effect of one structure. In the case of  $A+B$  the mixing is enhanced through the generation of small-scale

quasi-streamwise structures that are stretched in the streamwise direction as shown in Fig. 6. The interesting feature of these results is, once more, the localized character of mixing that can be indeed controlled. The parameters used here are not optimized yet, but the results we present prove clearly the feasibility of the process.

## CONCLUSION

A relatively new concept of active micro mixing has been introduced here. The mechanism is based on the interaction of induced vortical structures emerging from the action of wall actuators. The resulting quasi-streamwise (or horseshoe) vortices interact in a specific way to regenerate small vortical structures maintained by forcing. There are a number of parameters entering into the physics of the phenomena that needs to be studied in detail to obtain an optimum configuration for the spatial distribution of the wall actuators. This strategy is particularly suitable to enhance micro mixing locally in space and time while methods based on chaos results rather in global mixing.

The realization of the active process proposed here reveals to be technically feasible. Consider first the use of net zero mass flux jets for this purpose (Glezer and Amitay, 2002). The dimensions of the synthetic jet used here are typically  $d = 4a$  and  $d = 2a$  to engender respectively the structure  $A$  and  $B$ . Taking a microchannel flow with  $a = 200 \mu\text{m}$  results in  $d = 800 - 400 \mu\text{m}$  and the synthetic jets could be classified as mini rather than micro jets. The centerline jet velocity  $U_c$  for microchannel water flow at  $Re = 10$  is  $U_j = 0.05 \text{ m/s}$  under these circumstances. The maximum wall normal velocity corresponding to the perturbation parameters  $\varepsilon_A(t)$  and  $\varepsilon_B(t)$  reaches  $\langle v \rangle_{max} = \alpha U_c = 6 U_c$  during the oscillation cycle where  $U_c$  is the microchannel centerline velocity giving  $\langle v \rangle_{max} = 0.30 \text{ m/s}$ . Note that stable steady liquid jets with bulk velocity up to  $1.2 \text{ m/s}$  have been experimentally observed in hydrophobic microchannels of thickness  $100 \mu\text{m}$  (Huh et al., 2002) so that the break up phenomena is not questioned under the present circumstances. The maximum Reynolds number of the synthetic jet corresponding to the case investigated here is

$Re_j = \frac{\langle v \rangle_{max} d}{\nu} = 200$ . The Strouhal number describing how fast a fluid element leaves the orifice region is  $S = \frac{2\pi d}{T \langle v \rangle_{max}} = 0.6$  where  $T$  is the imposed period

( $T = 0.032 \text{ s}$  and the imposed frequency is  $f = 31 \text{ Hz}$ ). It is seen that the Reynolds and Strouhal numbers are respectively large and low enough to insure high momentum injection into the wall flow (Wu and Breuer, 2003). These elements show that the mixing strategy suggested here is technically feasible by means of synthetic jets. The use of coaxial jets could, on the other hand, easily lead to the formation of hairpin like vortices whose spanwise interactions enhance the mixing according to the mechanism we suggest here. Wall deformation actuators such as those used in the active wall turbulence control (Yoshino et al., 2002) can also be used after some miniaturization efforts. Both the tip displacement (up to  $90 \mu\text{m}$ ) and the resonant frequency (about  $500 \text{ Hz}$ ) of the seesaw type magnetic actuator realized later by the same

group are convenient although the size of the  $S_i$  flap is rather large (1 mm) (Yamagami et al., 2005). Finally temporal waveforms different than the sinusoidal one of either the synthetic jets or the wall deformation actuators have to be analyzed to determine the optimum excitation strategy to enhance the generation of turbulent like structures and mixing. In case of difficulties to implant active vortex generating methods, micro-patterning the electric surface charge to be locally positive, negative or neutral render possible the generation of electrokinetically formed single, co-rotating or counter rotating vortical structures, with the possibility of creating zones of streamwise vorticity (Lee et al., 2006). It is legitimate to expect enhanced mixing by imposing a spanwise asymmetry in the patterned surface charge technique. Our group will explore this possibility in the next future.

## REFERENCES

- Glezer A., Amitay M., 2002 "Synthetic jets" *Annu. Rev. Fluid Mech.*, 34, pp.503-529.
- Hessel V, Löwe H., Schöndel F, 2005 "Micro-mixers-a review on passive and active mixing principles" *Chem. Eng. Sci.* 60, pp. 2479-501.
- Henningson D.S., Lundbladh A., Johansson A., 1993 "A mechanism for bypass transition from localized disturbances in wall-bounded shear flows", *J. Fluid Mech.*, 250, 169-207
- Huh D., Wei H-W, Grotberg J.-B., Takayama S., 2002 "Development of stable and tunable high-speed liquid jets in microscale for miniaturized and disposable flow cytometry" 2<sup>nd</sup> Annual Int. IEEE-EMBS Special Topic Conference on Microtechnologies in Medicine&Biology, May 2-4, Madison, Wisconsin USA, pp. 449-452.
- J. Jeong, F. Hussain, 1995 "On the identification of a vortex" *J. Fluid Mech.*, 285, pp. 69-94
- Lee L.M., Lap W., Hau W., Lee Y-K., Zohar Y., 2006 « In-plane vortex flow in microchannels generated by electroosmosis with patterned surface charge" *J. Micromech. Microeng.* 16 17-26
- Tardu S., Nacereddine R., 2006 "Bypass transition through interactions of localized disturbances in wall bounded flows" To appear in *J. Non-linear Dynamics*.
- Tardu S., Nacereddine R., Doche O., 2006 "An interactive by-pass transition mechanism in wall bounded flows" Submitted to *J. Fluid Mech*.
- Tian F., Li, B., Kwok Y. 2005 "Tradeoff between mixing and transport for electroosmotic flow in heterogeneous microchannels with nonuniform surface potentials" *Langmuir*, 21 (3) pp. 1126-1131.
- Wu K.E., Breuer K.S., 2003 "Dynamics of synthetic jet actuator arrays" *AIAA Paper*, vol. 2003-4257.
- Yamagami T., Suzuki Y., Kasagi N., 2005 "Development of feedback control system of wall turbulence using MEMS devices" 6th Symp. on Smart Control of Turbulence Tokyo, Japan.
- Yoshino T., Tsuda M., Suzuki Y, Kasagi N. 2002 "Toward development of feedback control system for wall turbulence with MEMS sensors and actuators" 3rd Symp. on Smart Control of Turbulence Tokyo, March 3-5, 2002

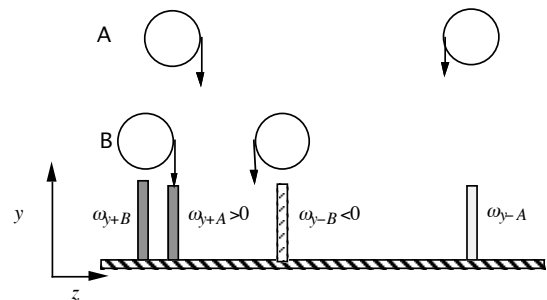


**Figure 1** Cross sectional view of two pairs of counter rotating quasi-streamwise vortices in the plane  $y-z$ . The pair  $A$  regenerates wall normal vorticity layers denoted by  $\omega_{y\pm A}$  positive and negative respectively at the left and the right. Similar vorticity layers  $\omega_{y\pm B}$  are generated by the pair  $B$ .

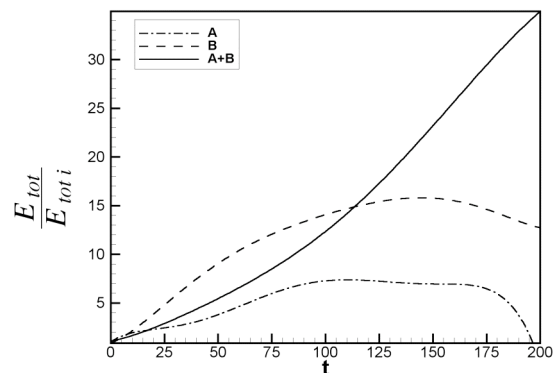


**Figure 2** Evolution of the total energy with imposed initial conditions at  $Re = 2000$ . See the text for further details.

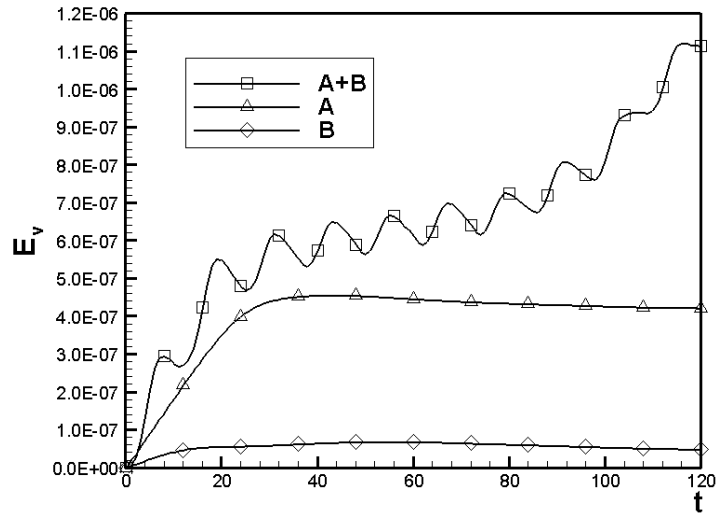


**Figure 3** Evolution of the wall normal velocity energy with time corresponding to unsteady forcing. See the text for details.

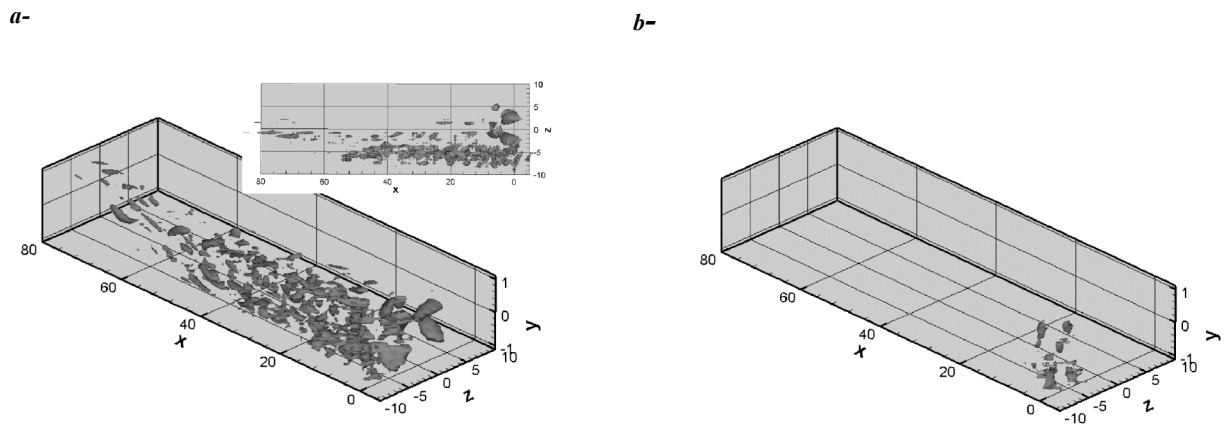
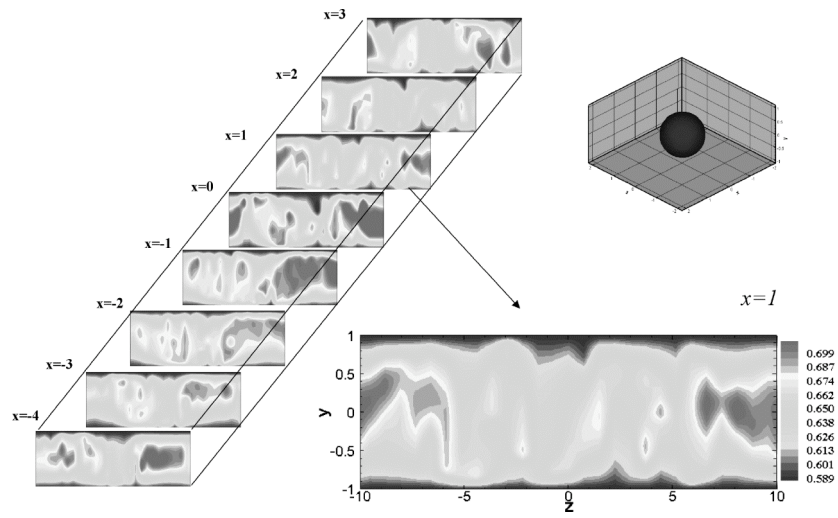


**Figure 4** Quasi-streamwise structures induced by the combination  $A + B$  (a) and  $B$  alone (b). For details see the text.

a



b-

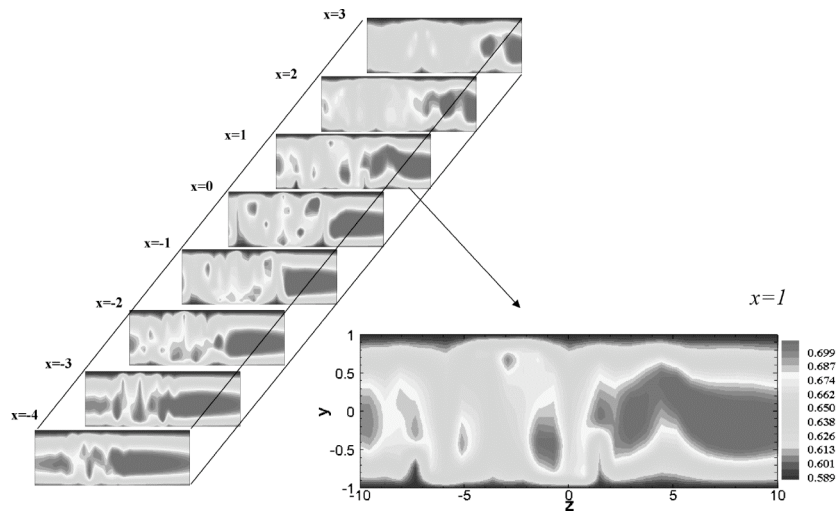


**Figure 5** Snapshots of the scalar in the  $y-z$  planes at  $t = 3$  and different streamwise positions while  $A$  interacts with  $B$  (a) and  $B$  alone (b). The initial scalar distribution is shown on right top of the Fig. The Reynolds number is  $Re = 10$ .

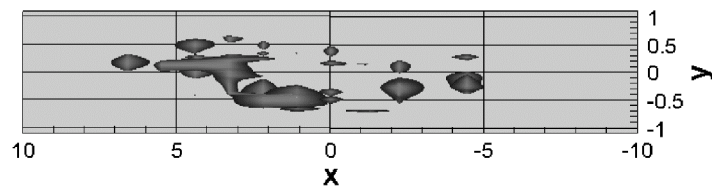


**Figure 6** High intensity structures detected by  $\lambda_2$  for the configuration  $A + B$  at  $t = 2$  ( $Re = 10$ )